11^{th} International Conference on Fracture Mechanics of Concrete and Concrete Structures
FraMCoS-11
J. M. Chandra Kishen, A. Ramaswamy, S. Ray and R. Vidyasagar (Eds)
https://doi.org/10.21012/FC11.092373

EFFECTS OF COUPLED CORROSION AND FATIGUE ON THE PERFORMANCE OF REINFORCED CEMENT CONCRETE

VIVEK VISHWAKARMA* AND SONALISA RAY†

*Indian Institute of Technology Roorkee
Roorkee, UK, India
e-mail: vivek_v@ce.iitr.ac.in

†Indian Institute of Technology Roorkee
Roorkee, UK, India
e-mail: sonalisa.ray@ce.iitr.ac.in

Key words: Reinforced cement concrete, Chloride diffusion, Coupled corrosion and fatigue, Corrosion

Abstract. Reinforced cement concrete is the most preferred material for load-bearing members in different structures like buildings, bridges, offshore structures, etc. A wide range of structures built in corrosive environments are also subjected to cyclic loads. Under the coupled effect of corrosion and fatigue, the structural performance significantly deteriorates, fatigue life gets reduced, and failure is sudden and without warning. In this study, a numerical analysis has been done to understand the behaviour of lightly reinforced cement concrete beam subjected to coupled conditions of corrosion and fatigue. The present study deals with the flexural behaviour of a single notched specimen of lightly reinforced cement concrete beam.

1 INTRODUCTION

Since the early age of its development, RCC has been considered a durable material due to the chemical inertness of concrete and its capabilities to protect steel from oxidation. But later, it was established that oxidation of reinforcement steel, i.e., corrosion is an eminent process, and it is a continuous process during the service life of a structure.

Chloride ion ingress and carbonation are the two most damaging factors for reinforcement corrosion in RCC structures. Carbonation causes uniform corrosion, whereas chloride ion diffusion cause both pitting corrosion and general corrosion. Expansive corrosion products are formed during the corrosion, leading to increased volumetric strain in concrete with subsequent bond failure, cracking, and spalling of concrete cover. Corrosion of rebar causes a decrease in load carrying capacity of RCC members and hence leads to decreased serviceability and durability. Sometimes this localized corrosion, termed as pitting corrosion, takes place and does not have any visible effects on the structural member. However, due to local reduction in rebar area, stress concentration becomes a dominant factor for the failure of that member. Fatigue cracks usually initiate and propagate from these corrosion pits. Numerous structures, which include offshore structures, RCC bridges, mobile drilling structures, etc., are subjected to cyclic loading, combined with corrosion of reinforcing steel. This combined effect of cyclic loading along with the corrosion of reinforcement is known as coupled corrosion fatigue, in which the premature and sudden failure of the structure has been observed.

Both, corrosion due to chloride ion ingress and fatigue loads are complementary loads and have a harmonious effect on the performance of RCC members. Cyclic load causes early-age cracking in concrete, accelerating the chloride ion transport. Enhanced availability of oxygen and moisture in the vicinity of these cracks results in the formation of corrosion pits and further cracking of concrete cover.

The present work is focused on the experimental investigation of reinforced concrete beams under constant amplitude cyclic loads of varying stress ratios to determine the parameters required for numerical modelling and the numerical investigation of similar beams under the action of coupled corrosion fatigue.

2 LITERATURE REVIEW

A passive film is generated around the surface of the rebar due to the high alkalinity of the concrete pore solution. The high pH of concrete prevents the steel from active electrochemical corrosion. But in aggressive environments like marine structures or areas with high humidity, the ingress of active ions like chloride or sulphate ions can destroy the passive file by reducing the pH of concrete pore solution [1]. As the volume of corrosion products varies from 2 to 6 times of original steel volume corroded [2]. Additional volumetric strains are generated from corroded steel as the rebar is confined by concrete, causing cracking, spalling, or delamination of concrete covers [3]. Subsequently, the load-bearing capacity of RCC elements decreases, affecting their durability and safety [4]. Accumulation of corrosive product on the surface of rebar results in the reduction of rebar-concrete bond strength [5].

Generally, the existing steel corrosion models can be divided into three groups [6]: the empirical model, the reaction control model, and the electro-chemical model. Corrosion of steel in concrete is a dynamic and continuous interaction between steel, corrosion products, and concrete. Numerical modeling of corrosion is difficult due to interdependency of several factors on each other [7]. Anode and cathode cell area optimization is very complex and still an open field in the corrosion of reinforcement in concrete [8]. Attempts have been made to simulate the structural effects of corrosion reaction through cracked concrete and its consequences for corrosion-induced damage [9].

Natural corrosion of rebar is generally a slow process and not feasible to study for laboratory purposes. The impressed current technique is the most popular technique for accelerated corrosion. However, the corrosion behavior of steel under artificial conditions is different from those in natural environments [10]. Nevertheless, the impressed current method has some advantages over natural corrosion and artificial climate environment method, including short acceleration duration and high repeatability.

Fatigue is a process of progressive, permanent damage taking place in the structural member due to cyclic loads [11–13]. Fatigue study in reinforced concrete is much more complex due to the heterogeneity of concrete and the interaction of concrete and steel [14]. Fatigue strength behavior of the RCC beam depends on factors like fracture mode, crack growth, the relationship between loading, stirrup strains, etc. Given the importance of the steel-concrete bond, the crack extension in RC structures has been widely studied using several crack models, including the discrete crack model [15], the cohesive crack model [16], and numerical methods using FEA [17]. To date, closed-form analytical solutions have received the researcher's interest and are broadly classified into two groups: the force-balance-based and fracture-based methods.

A study on the crack extension process in lightly reinforced members with bond-slip behavior is still insufficient due to the following two reasons. First, the assumption of plane-section assumed in the force balance method is no longer valid in the presence of reinforcement. Second, for the fracture mechanics-based analytical model, the bond behavior is either ignored or simplified by the empirical formula [18]. In conjunction with fracture mechanics, the theory of dimensional analysis can be used

to study fatigue crack propagation [19]. Few researchers have studied fatigue crack growth propagation using acoustic emission [20–23]. The acoustic emission technique captures the elastic waves propagating in the material due to damage like crack formation, propagation, and damage classification. The RCC structures are more susceptible to fatigue damage accumulation, coupled with reinforcement corrosion, which significantly deteriorates the performance of RCC structures [24]. Stress concentration induced by pitting corrosion damage of the rebar will result in premature fatigue crack nucleation [25].

In order to include the corrosion pit growth in fatigue analysis, various models have been proposed; most researchers considered corrosion pits as an initial crack on the surface [26]. Different notch shapes have been considered for the analysis and their validity as a notch for applying fracture mechanics [27]. The Equivalent Initial Flaw Size (EIFS) methodology has been used to predict service life for smooth and notched specimens without corrosion effects [26,28]. When corrosion and fatigue occur together, damage to the bond interface induced by corrosion may lead to a decrease in fatigue resistance and accelerate fatigue damage. Limited experimental studies have been conducted on the coupled effects of corrosion and fatigue loading. Limited experimental studies available in the literature concluded that cracking pattern, and coupled effects significantly affect flexural stiffness [29, 30]. The effect of fatigue loads, corrosion current, and loading frequency is studied to assess the joint effect on the flexural performance of RCC beams [31].

A closed form analytical solution to the problem of coupled corrosion and fatigue is yet not available due to the non-linearity and heterogeneity of concrete. The aim of this study is to utilize the available models to get acceptable results for the above-said load case.

3 EXPERIMENTAL PROGRAM

3.1 Material properties

43-grade ordinary Portland cement is used to cast the concrete beam specimen. Mix design is done according to IS 10262:2009. Locally available river sand is used with specific gravity of 2.59, maximum size of coarse aggregate is 10 mm. The mix proportion details and properties of various ingredients used in the preparation of concrete, are summarized in Table 1 The average 28-day cube compressive strength of standard size is 38 N/mm^2. Deformed bars of grade Fe 550SD are used as reinforcement in the beam specimen having measured yield strength of 600 N/mm^2. The beams of dimensions $1000mm \times 200mm \times 120mm$ are cast and cured for 28 days. Further, a 3 mm width notch of length 30 mm is saw cut on the 25th day of curing. The reinforcement ratio is designed according to criteria given by Bosco and Carpinteri [32].

Table 1: Details of concrete mix and material properties

w/c , (mm)	0.45
Mix proportion	1:1.74:2.2
f_{ck}	38 N/mm^2
Tensile strength (ft)	3.7 N/mm^2
Poisson's ratio (ν)	0.2
Young's Modulus (E)	33980 N/mm^2

3.2 Test Setup

The beams are tested under center point loading with a constant amplitude cyclic load of varying load ratios. All tests have been done on a 500 kN closed-loop servo-controlled fatigue testing machine. Typical geometry of the beam is shown in figure 1

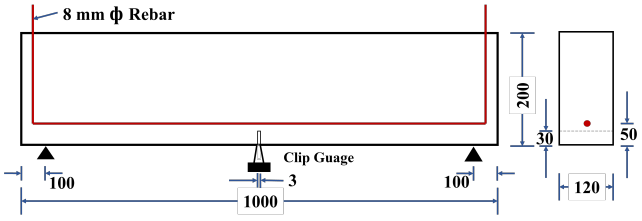

Figure 1: Details of the geometry of lightly reinforced beam.

The crack mouth opening displacement (CMOD) is measured using a clip gauge. Initially, the beam specimens are tested under CMOD-controlled monotonic load to determine the static load capacity of the beam. The beam specimens are tested under constant amplitude cyclic load of stress ratio R as 0.5 to 0.8. The loading frequency is maintained at 2 Hz for all the tests. To ensure proper contact, the minimum load is kept at 2 kN. The data of load, CMOD, and loading point displacement is acquired.

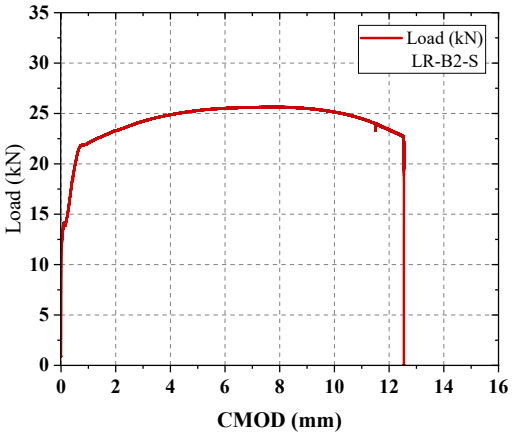

Figure 2: Load vs CMOD under monotonic load

3.3 Experimental Results

The average peak load capacity of three beams tested under CMOD control monotonically increasing load is 27 kN with a standard deviation of 0.85. The load vs CMOD and Load vs Deflection plot is presented in Figure 2 and Figure 3.

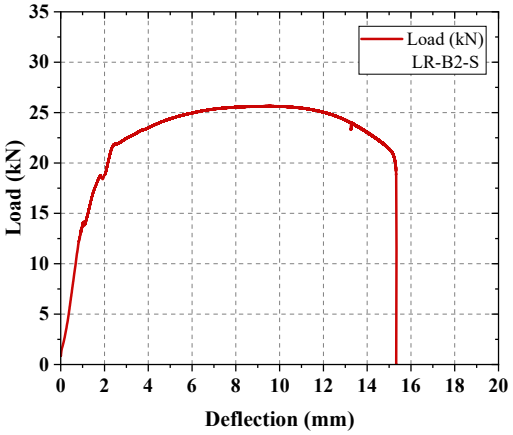

Figure 3: Load vs Deflection under monotonic load

The fatigue test has been performed three beam specimens as per section 3.2 at frequency of 2 Hz with the load ratio (R) of 0.5, 0.6, 0.7 and 0.8. The average fatigue life of specimens under different load ratio are shown in Table 2.

A typical peak-valley curve of CMOD and deflection vs no. of cycles of specimen LR-B12-C7 with R = 0.7 is presented in Figure 4 and Figure 5. Peak CMOD and valley CMOD are defined as the maximum and minimum CMOD observed respectively, for each cycle throughout the test. Similarly, peak deflection and valley deflection is defined as the maximum and minimum deflection observed respectively, for each cycle throughout the test.

Table 2: Average No. of cycles till failure under varying load ratio

S. No.	Load Ratio	Max Load (kN)	N_f
1	0.5	13.5	364500
2	0.6	16.2	163446
3	0.7	18.9	47420
4	0.8	21.6	27000

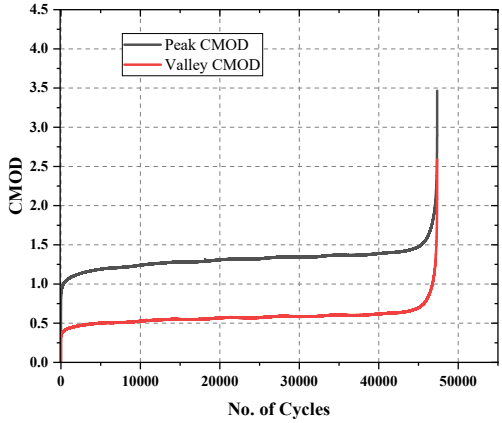

Figure 4: Peak-Valley CMOD vs No. of cycles (R = 0.7)

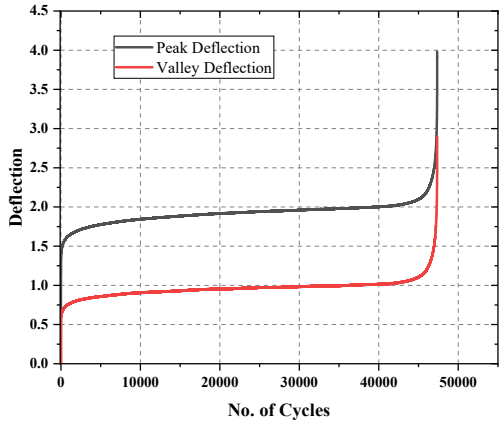

Figure 5: Peak-Valley Deflection vs No. of cycles (R = 0.7)

4 NUMERICAL INVESTIGATION

Numerical analysis has been performed to understand the behaviour of reinforced concrete beams under coupled action of corrosion and fatigue. A similar lightly reinforced beam is modelled in commercially available finite element software ATENA to simulate the behaviour under the action of the following load cases;

- Under static loading in the corrosive environment
- Under repetitive loading in ambient conditions
- Under repetitive loading in a corrosive environment representing the coupled phenomena of corrosion-fatigue

The beam has a notch of depth of 30 mm and a width of 3 mm at the bottom center. Concrete is modelled with material properties as shown in Table 3

$\beta_{fatigue}$ and ξ_{COD} are fatigue parameters as described by Cervenka et al. [33]. ATENA uses a fracture-plastic model modified to make it suitable for analyzing the fatigue behaviour of concrete. It uses a stress-based model. $\beta_{fatigue}$ and ξ_{COD} are the additional parameters required for damage calculation due to stresses and crack opening closing, respectively. These parameters have been calibrated using experimental data. Reinforcement is modelled as a 1D element; its model parameters are listed in Table 4. The chloride boundary condition is applied at appropriate analysis intervals with the parameters listed in Table 5.

The chloride model implemented in ATENA is one-dimensional diffusion-based law which is divided into three parts, namely the diffusion phase till the corrosion initiation, propagation phase, and concrete cracking phase [9].

Table 3: Model parameters for concrete

Compressive strength, $f_c\ (N/mm^2)$	38
Tensile strength, $f_t\ (N/mm^2)$	4
Young's modulus, $E\ (N/mm^2)$	34000
Fracture energy, $G_F\ (N/m)$	130
Max. Size of aggregate, (mm)	10
$\beta_{fatigue}$	0.05
ξ_{COD}	0.0001

Table 4: Model parameters for reinforcement steel

Diameter of bar (mm)	Yield strength $f_y\ (N/mm^2)$	Yield strain
8	600	0.0025

The initiation model is based on the assumption mentioned in DuraCrete model, that the corrosion of steel starts at the time when the

chloride content exceeds the critical chloride content, (Cl_{crit}).

$$C(x,t) = C_s \left[1 - erf\left(\frac{x}{2\sqrt{D_m(t)f(w)t}}\right)\right] \quad (1)$$

where C_s is the chloride content applied at the boundary (kg of chlorides/kg of a binder), $D_m(t)$ is the mean (averaged) diffusion coefficient at the time t (m^2/s) [34]. x is the distance from the loaded surface (m) and $f(w)$ includes the effect of crack width w (mm)

$$f(w) = 31.61w^2 + 4.73w + 1 \quad (2)$$

The propagation phase is modelled using Liu and Weyer's model [35]. the corrosion rate is related to corrosion current density (i_{corr}) and Faraday's Law

$$i_{corr} = 0.926 \times exp\,[7.98 + 0.7771ln(1.69 \times C_{M,binder}) - \frac{3006}{T} - 0.000116R_c + 2.24t^{-0.215} \quad (3)$$

Further, the cracking of concrete is estimated using DuraCrete Model. The critical depth of penetration of oxides formed during corrosion reaction is formulated as

$$x_{corr,cr} = a_1 + a_2\frac{C}{d_{ini}} + a_3 f_{t,ch} \quad (4)$$

where the a_1, a_2 and a_3 are fixed parameters, C is thickness of cover in metres. d_{ini} in the initial diameter of reinforcement bar and $f_{t,ch}$ is characteristic splitting tensile strength of concrete in $N/mm2$. The model is meshed with structured hexahedra elements of size 10 mm. The analysis is carried out using a fracture-plastic model, which can include the aggregate size effect, crack spacing, tension stiffening, etc.

Table 5: Parameters for Cl boundary condition

Diffusion coefficient,$D_{ref}(m^2/Day)$	1.37e-7
m_{coeff}	0.66
Surface chloride concentration,(C_s)	5%
Critical chloride concentration,(Cl_{crit})	0.5%
Rate after spalling, $(mm/year)$	0.003

Load vs deflection plot of monotonic load is presented in Figure 6. The flexural capacity of the beam under a three-point monotonically increasing load is 29 kN which is near to the observed experimental flexural capacity of 27 kN as mentioned in section 3.3

Further, the lightly reinforced beam is simulated for fatigue loads having varying stress ratios, i.e., R = 0.5,0.6,0.7,0.8. Load-controlled analysis has been performed with a maximum load equal to R times the peak static load and a minimum load equal to zero. In ATENA, fatigue damage is evaluated for a user-defined number of cycles. For the present simulation, fatigue damage is applied in cycles over a series of 1000, 2000, 4000, 8000, 16000, and so on till failure. Load vs deflection curve for the plain fatigue load having R = 0.7 is presented in Figure 7 and for the coupled corrosion and fatigue load having R = 0.7 is presented in Figure 8. The corrosion profile of the reinforcement bar for the coupled case is shown in figure 9. Table **??** and Table 7 provides a consolidated summary of numerical results for different load ratio.

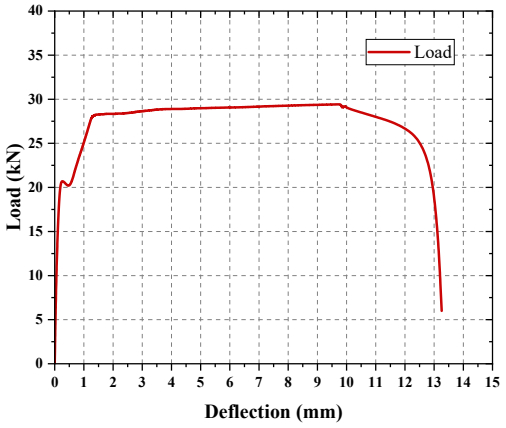

Figure 6: Load vs deflection plot for monotonic load

Table 6: No. of cycles completed before failure under varying load ration

Load ratio	N_f Only fatigue	N_f Coupled load	% Reduction
0.5	256000	160000	37.5
0.6	140000	80000	42
0.7	40000	27000	32
0.8	24000	14000	41

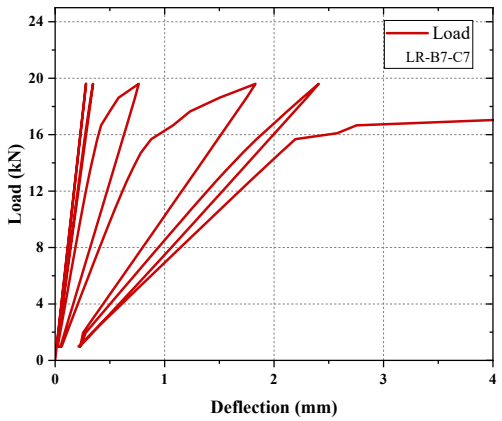

Figure 7: Cyclic Load vs Deflection curve of lightly reinforced beam R = 0.7

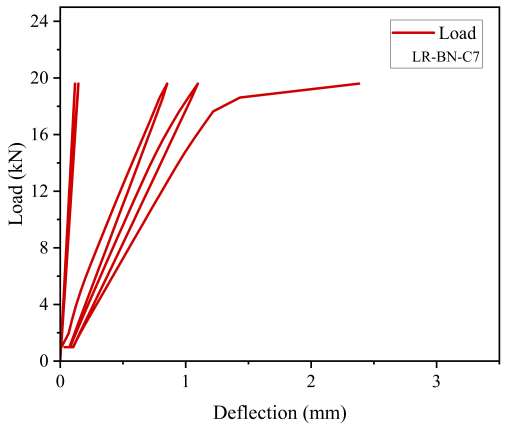

Figure 8: Cyclic Load vs Deflection curve of lightly reinforced beam R = 0.7 in coupled condition

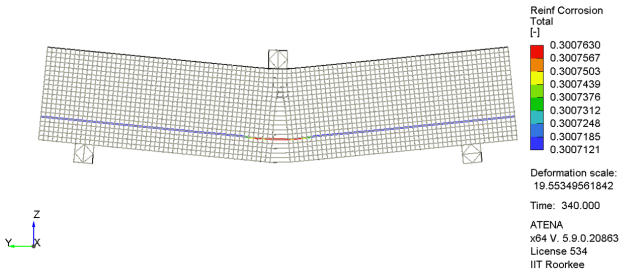

Figure 9: Corrosion profile and mass loss in coupled loading conditions

Table 7: Corrosion mass loss in coupled loading condition under different stress ratio

Load ratio	Corrosion mass loss
0.5	0.27
0.6	0.28
0.7	0.31
0.8	0.36

5 CONCLUSIONS

The effects of corrosion and fatigue loads are complementary to each other. Crack formation in cyclic loads leads to enhanced corrosion. The following conclusions are drawn from the present study:

- Fatigue failure in lightly reinforced concrete beams progresses in three phases. Initially, peak deflection increases rapidly till the crack reaches near the mid-depth, In the second phase, beam behaves like an elastic member due to the reinforcement. In the later stages, the beam fails suddenly due to fatigue failure of the reinforcement bar.

- The peak deflection in the case of fatigue load is significantly smaller than the deflection recorded in the monotonic load case.

- In coupled loading conditions, the fatigue performance of the beam is significantly degraded. The average reduction in no.

of cycles to failure is about 38 % and failure take place at lesser deflection than the plain fatigue condition.

- As the load ratio is reduced, the maximum corrosion percentage is also reduced due to less crack opening in lower load ratios. The reinforcement near the crack is subjected to higher chloride concentration and hence non-uniform corrosion is observed.

Acknowledgment

Authors are grateful to acknowledge the financial support provided by the Science and Engineering Research Board, New Delhi through research grant number SER-1700-CED For the present study.

REFERENCES

[1] Y.F. Cheng and J.L. Luo. Electronic structure and pitting susceptibility of passive film on carbon steel. *Electrochimica Acta*, 44(17):2947–2957, 1999.

[2] Arto Köliö, Mari Honkanen, Jukka Lahdensivu, Minnamari Vippola, and Matti Pentti. Corrosion products of carbonation induced corrosion in existing reinforced concrete facades. *Cement and Concrete Research*, 78:200–207, 2015.

[3] Carmen Andrade. Propagation of reinforcement corrosion: principles, testing and modelling. *Materials and Structures*, 52(1), 2 2019.

[4] Hailong Ye, Chuanqing Fu, Ye Tian, and Nanguo Jin. *Chloride-Induced Steel Corrosion in Concrete Under Service Loads*. 1 2020.

[5] Yuxi Zhao, Jiang Yu, Bingyan Hu, and Weiliang Jin. Crack shape and rust distribution in corrosion-induced cracking concrete. *Corrosion Science*, 55:385–393, 2 2012.

[6] Feng Xu, Xiao Yifei, Shu-Guang Wang, Weiwei Li, Weiqing Liu, and Dongsheng Du. Numerical model for corrosion rate of steel reinforcement in cracked reinforced concrete structure. *Construction and Building Materials*, 180:55–67, 8 2018.

[7] Joško Ožbolt, Gojko Balabanić, and Marija Kušter. 3D Numerical modelling of steel corrosion in concrete structures. *Corrosion Science*, 53(12):4166–4177, 12 2011.

[8] Joško Ožbolt, Filip Oršanić, Gojko Balabanić, and Marija Kušter. Modeling damage in concrete caused by corrosion of reinforcement: coupled 3D FE model. *International Journal of Fracture*, 178(1-2):233–244, 10 2012.

[9] Kateřina Hájková, Vít Šmilauer, Libor Jendele, and Jan Červenka. Prediction of reinforcement corrosion due to chloride ingress and its effects on serviceability. *Engineering Structures*, 174:768–777, 11 2018.

[10] Jinwei Chen, Chuanqing Fu, Hailong Ye, and Xianyu Jin. Corrosion of steel embedded in mortar and concrete under different electrolytic accelerated corrosion methods. *Construction and Building Materials*, 241:117971, 4 2020.

[11] Bineet Kumar and Sonalisa Ray. A multiscale based fracture characterization in concrete under fatigue loading using critical energy dissipation. *International Journal of Fatigue*, 165:107165, 2022.

[12] Bineet Kumar and Sonalisa Ray. An analytical approach for the fracture characterization of concrete under cyclic loading. *Materials Today: Proceedings*, 2023.

[13] Bineet Kumar and Sonalisa Ray. Nanomechanics based crack growth characterization of concrete under fatigue loading.

Procedia Structural Integrity, 39:222–228, 2022.

[14] M. H. Prashanth, Parvinder Pal Singh, and J.M. Chandra Kishen. Role of longitudinal reinforcement on the behavior of under reinforced concrete beams subjected to fatigue loading. *International Journal of Fatigue*, 125:271–290, 8 2019.

[15] Gonzalo Ruiz, Jacinto Ruiz Carmona, and David A. Cendón. Propagation of a cohesive crack through adherent reinforcement layers. *Computer Methods in Applied Mechanics and Engineering*, 195(52):7237–7248, 11 2006.

[16] Timon Rabczuk, Goangseup Zi, Stéphane Bordas, and Hung Nguyen-Xuan. A geometrically non-linear three-dimensional cohesive crack method for reinforced concrete structures. *Engineering Fracture Mechanics*, 75(16):4740–4758, 11 2008.

[17] Zhenwei Yang and Jian Fei Chen. Finite element modelling of multiple cohesive discrete crack propagation in reinforced concrete beams. *Engineering Fracture Mechanics*, 72(14):2280–2297, 9 2005.

[18] Yanjie Wang, Zhimin Wu, Jianjun Zheng, Rena C. Yu, and Yang Liu. Analytical method for crack propagation process of lightly reinforced concrete beams considering bond-slip behaviour. *Engineering Fracture Mechanics*, 220:106654, 10 2019.

[19] Sonalisa Ray and J.M. Chandra Kishen. Analysis of fatigue crack growth in reinforced concrete beams. *Materials and Structures*, 47(1-2):183–198, 1 2014.

[20] Santosh K. Shah and J.M. Chandra Kishen. Use of acoustic emissions in flexural fatigue crack growth studies on concrete. *Engineering Fracture Mechanics*, 87:36–47, 6 2012.

[21] R. Vidya Sagar and B. K. Raghu Prasad. Damage limit states of reinforced concrete beams subjected to incremental cyclic loading using relaxation ratio analysis of AE parameters. *Construction and Building Materials*, 10 2012.

[22] Noorsuhada Md Nor, Azmi Ibrahim, Norazura Muhamad Bunnori, Hamidah Mohd Saman, Soffian Noor Mat Saliah, and Shahiron Shahidan. Diagnostic of fatigue damage severity on reinforced concrete beam using acoustic emission technique. *Engineering Failure Analysis*, 41:1–9, 6 2014.

[23] N Md Nor, Shahrir Abdullah, and Soffian Noor Mat Saliah. On the need to determine the acoustic emission trend for reinforced concrete beam fatigue damage. *International Journal of Fatigue*, 152:106421, 11 2021.

[24] Yafei Ma, Yibing Xiang, Lei Wang, Jianren Zhang, and Yongming Liu. Fatigue life prediction for aging RC beams considering corrosive environments. *Engineering Structures*, 79:211–221, 2014.

[25] Shan Xu and You Wang. Estimating the effects of corrosion pits on the fatigue life of steel plate based on the 3D profile. *International Journal of Fatigue*, 72:27–41, 3 2015.

[26] Yibing Xiang and Yongming Liu. EIFS-based crack growth fatigue life prediction of pitting-corroded test specimens. *Engineering Fracture Mechanics*, 77(8):1314–1324, 5 2010.

[27] KK Sankaran, R Perez, and KV Jata. Effects of pitting corrosion on the fatigue behavior of aluminum alloy 7075-t6: modeling and experimental studies. *Materials Science and Engineering: A*, 297(1-2):223–229, 2001.

[28] Yibing Xiang, Zizi Lu, and Yongming Liu. Crack growth-based fatigue life prediction

using an equivalent initial flaw model. part i: Uniaxial loading. *International Journal of Fatigue*, 32(2):341–349, 2010.

[29] Emilio Bastidas-Arteaga, Philippe Bressolette, Alaa Chateauneuf, and Mauricio Sánchez-Silva. Probabilistic lifetime assessment of RC structures under coupled corrosion–fatigue deterioration processes. *Structural Safety*, 31(1):84–96, 1 2009.

[30] Wha-Seung Ahn and D. Nageshwar Reddy. Galvanostatic testing for the durability of marine concrete under fatigue loading. *Cement and Concrete Research*, 31(3):343–349, 3 2001.

[31] Yiyan Lu, Tang Wenshui, Shan Li, and Mingyong Tang. Effects of simultaneous fatigue loading and corrosion on the behavior of reinforced beams. *Construction and Building Materials*, 181:85–93, 8 2018.

[32] Crescentino Bosco and Alberto Carpinteri. Fracture mechanics evaluation of minimum reinforcement in concrete structures. In *Applications of fracture mechanics to reinforced concrete*, pages 347–378. CRC Press, 2018.

[33] Jan Cervenka. Modelling of high-cycle fatigue crack growth in concrete. 6 2019.

[34] Seung Jun Kwon, Ung Jin Na, Sang Soon Park, and Sang Hwa Jung. Service life prediction of concrete wharves with early-aged crack: Probabilistic approach for chloride diffusion. *Structural Safety*, 31(1):75–83, 2009.

[35] Y Liu and E Weyers. Modeling the Dynamic Corrosion Process in Chloride Contaminated Concrete Structures. *Cement and Concrete Research*, 28(3):365–379, 1998.